**Fig. S1**

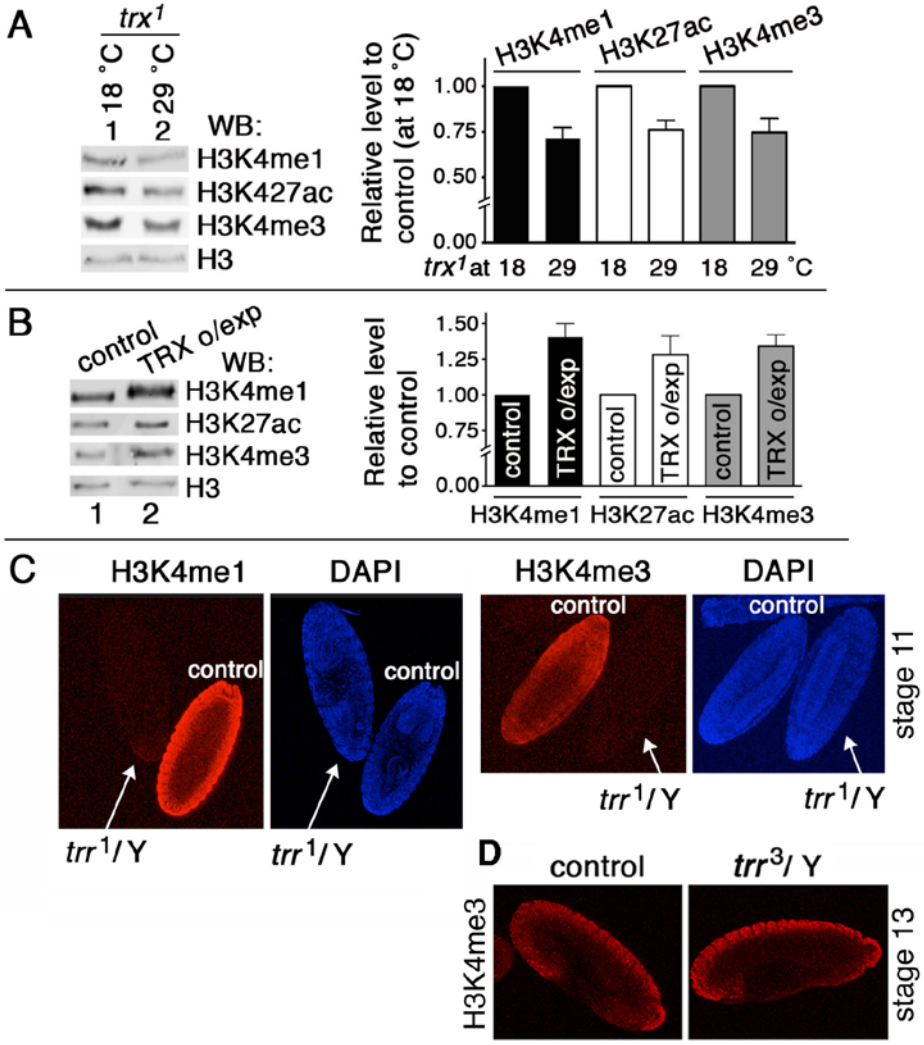
A
trx1
18 °C
29 °C
1
2
WB:
H3K4me1
H3K427ac
H3K4me3
H3
Relative level to control (at 18 °C)
H3K4me1
H3K27ac
H3K4me3
1.00
0.75
0.50
0.00
trx1 at 18 29 18 29 18 29 °C
B
control
TRX o/exp
WB:
H3K4me1
H3K27ac
H3K4me3
H3
1 2
Relative level to control
1.50
1.25
1.00
0.75
0.00
control
TRX o/exp
H3K4me1 H3K27ac H3K4me3
C
H3K4me1
DAPI
H3K4me3
DAPI
control
trr1/Y
stage 11
D
control
trr3/ Y
H3K4me3
stage 13

**Fig. S1. The *trx*$^{1}$ and *trr*$^{1}$ mutants and TRX over-expression affect both H3K4me1 and H3K4me3 levels.** (A and B) Histone H3 in salivary glands from *trx*$^{1}$ raised at 18 (control) or 29˚C in A and from TRX over-expresser in B (*w*$^{1118}$ as control) were analyzed by quantitative western. Standard error bars were calculated from three independent samples. (C) Immunostaining of wild-type (*w*$^{1118}$) and *trr*$^{1}$/Y mutant embryos (at stage 11) with anti-H3K4me1 and anti-H3K4me3 antibodies. *trr*$^{1}$/Y mutant embryos were indicated by arrows. DAPI staining indicates embryo position. (D) Immunostaining of wild-type (*w*$^{1118}$) and *trr*$^{3}$/Y mutant embryos (at stage 13) with anti-H3K4me3 antibodies. Note that the H3K4me3 level in *trr*$^{3}$/Y mutant embryos was unchanged.

**Fig. S2**

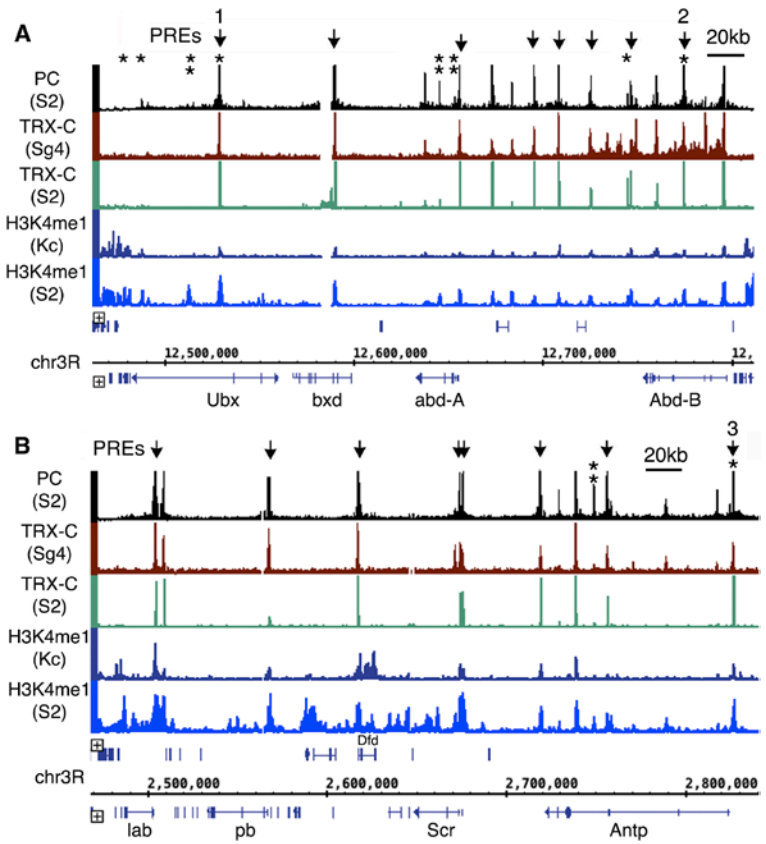


**Fig. S2. H3K4me1 and TRX-C are enriched at PREs.** Plots of PC in *Drosophila* S2 cells (Tie et al., 2012), TRX-C in Sg4 (Schwartz et al., 2010) and S2 cells (Enderle et al., 2011), H3K4me1 in Kc (Kellner et al., 2012) and S2 cells (Herz et al., 2012) are shown for the *Bithorax* (in A) and *Antennapedia* Complexes (in B). Arrows indicate known PREs. Enhancers of *Ubx*, *abd-A*, *Abd-B* and *Antp* identified by STARR-seq in S2 cells (Arnold et al., 2013) are indicated by asterisk (strong enhancer with double asterisks). Note that H3K4me1 and TRX-C peaks are present at all PREs. Note that three enhancers (marked by 1 and 2 in A, and 3 in B) are close to or overlap at PREs.

**Fig. S3**

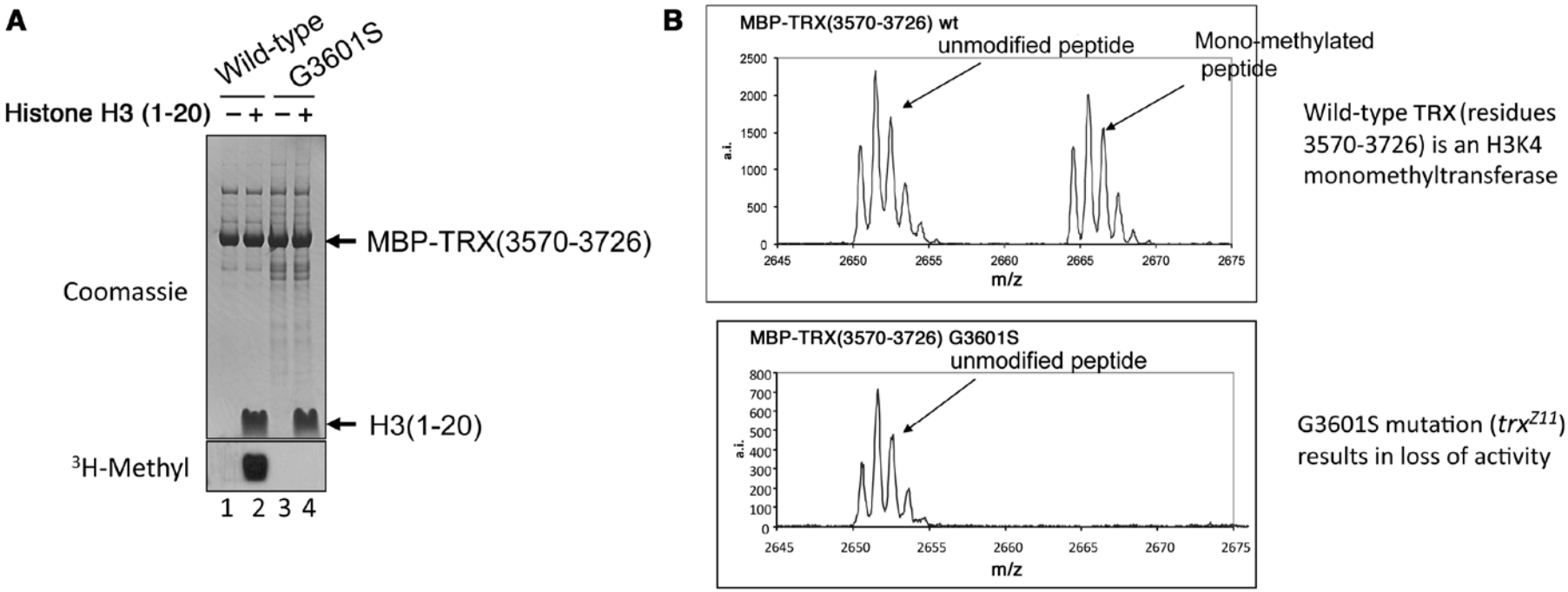


**Fig. S3. TRX SET is an H3K4 monomethyltransferase in vitro.** (**A**) In vitro histone methyltransferase (HMT) assay. TRX SET domain (wild type and G3601S mutant as indicated at top of each lane) and radioactive $^{3}$H-methyl were used in HTM assay with peptide histone H3 (1-20) as substrate. **(B**) G3601S mutation (*trx*$^{Z11}$) abolishes the H3K4 monomethylation activity of TRX. Peptides of H3 (1-20) after HMT assay above were analyzed by MALDI TOF mass spectrometry. Note that monomethylated peptide when using wild type TRX (top) disappeared when using G3601S mutation (bottom).

**Fig. S4**

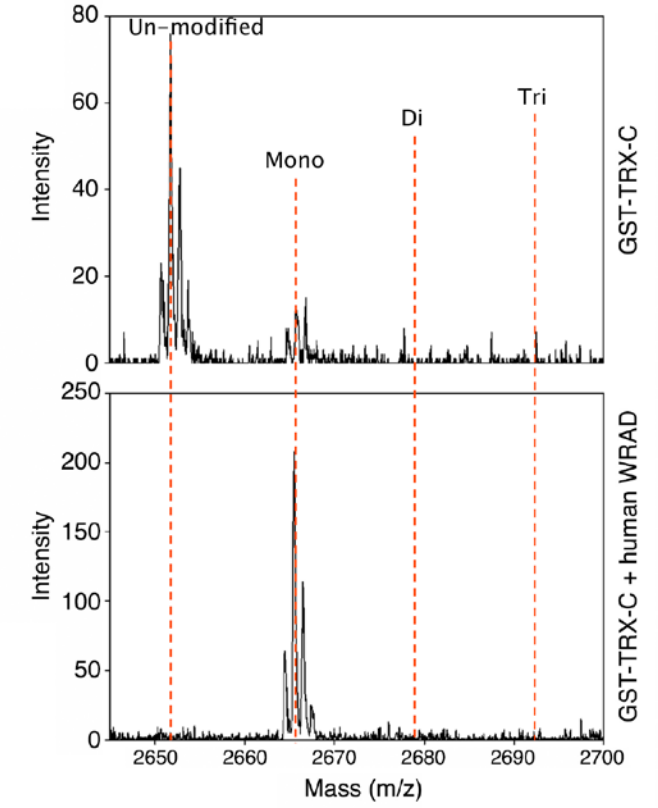


**Fig. S4. WRAD (WDR5, RbBP5, Ash2L, and DPY-30) components of MLL1 core complex dramatically enhance H3K4 monomethylation by TRX but have no change on product specificity.** GST-TRX-C251 (residues 3476-3726) (top) or GST-TRX-C251 in a stoichiometric complex with human WRAD components (bottom) and histone H3(1-20) peptide were used in vitro HMT assays. Products were measured by quantitative MALDI-TOF mass spectrometry as previously described (Patel et al., 2009). Note that while approximate 90% of H3 peptide is unmodified and 10% is monomethylated in top panel (using GST-TRX-C), ~100% of H3 peptide is monomethylated in the lower panel (using GST-TRX-C + human WRAD).

**Fig. S5**

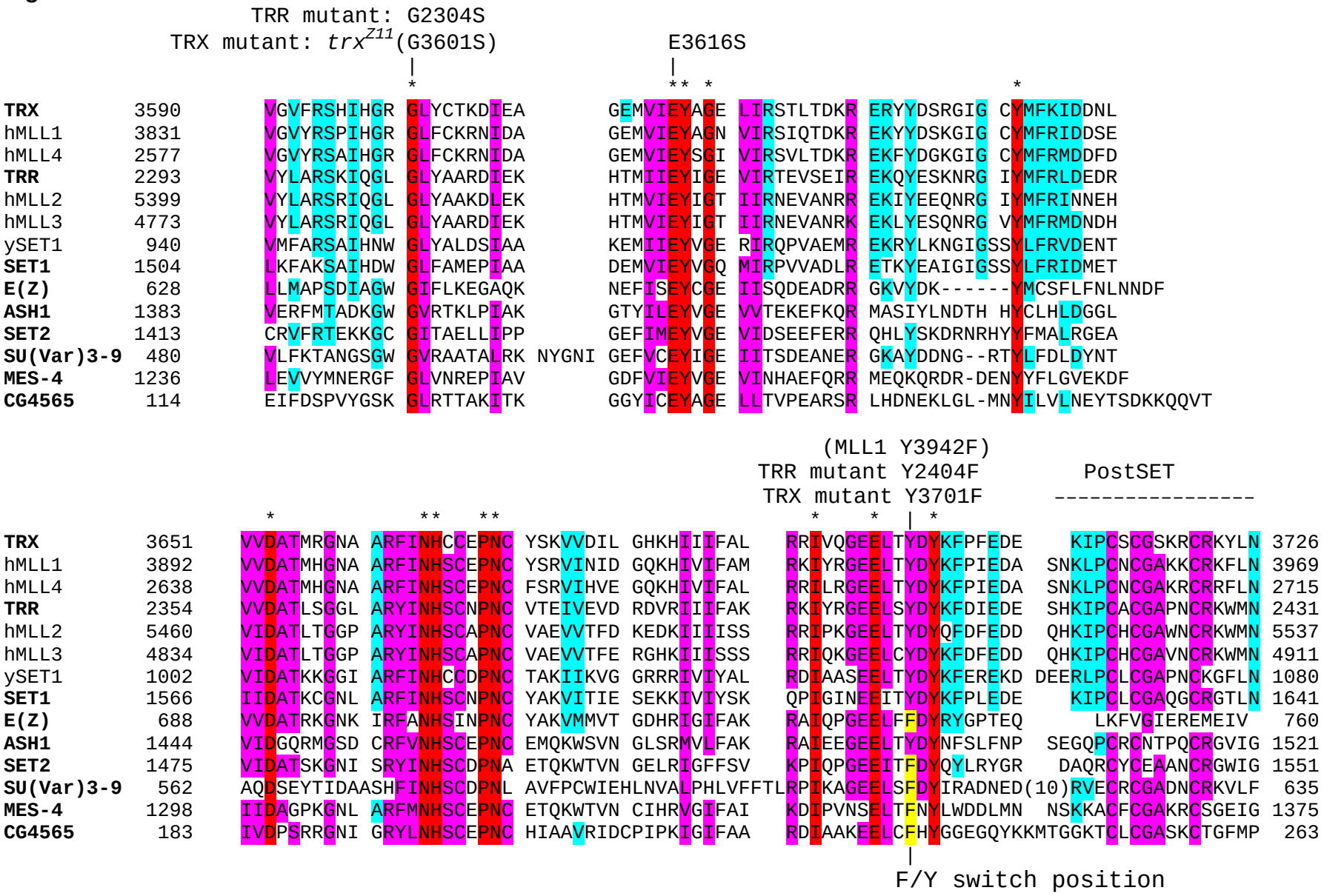
TRR mutant: G2304S
TRX mutant: trx^Z11(G3601S)
E3616S
TRX 3590 VGVFRSHIHGR GLYCTKDIEA GEMVIEYAGE LIRSTLTDKR ERYYDSRGIG CYMFKIDDNL
hMLL1 3831 VGVYRSPIHGR GLFCKRNIDA GEMVIEYAGN VIRSIQTDKR EKYYDSKGIG CYMFRIDDSE
hMLL4 2577 VGVYRSAIHGR GLFCKRNIDA GEMVIEYSGI VIRSVLTDKR EKFYDGKGIG CYMFRMDDFD
TRR 2293 VYLARSKIQGL GLYAARDIEK HTMIIEYIGE VIRTEVSEIR EKQYESKNRG IYMFRLDEDR
hMLL2 5399 VYLARSRIQGL GLYAAKDLEK HTMVIEYIGT IIRNEVANRR EKIYEEQNRG IYMFRINNEH
hMLL3 4773 VYLARSRIQGL GLYAARDIEK HTMVIEYIGT IIRNEVANRK EKLYESQNRG VYMFRMDNDH
ySET1 940 VMFARSAIHNW GLYALDSIAA KEMIIEYVGE RIRQPVAEMR EKRYLKNGIGSSYLFRVDENT
SET1 1504 LKFAKSAIHDW GLFAMEPIAA DEMVIEYVGQ MIRPVVADLR ETKYEAIGIGSSYLFRIDMET
E(Z) 628 LLMAPSDIAGW GIFLKEGAQK NEFISEYCGE IISQDEADRR GKVYDK------YMCSFLFNLNNDF
ASH1 1383 VERFMTADKGW GVRTKLPIAK GTYILEYVGE VVTEKEFKQR MASIYLNDTH HYCLHLDGGL
SET2 1413 CRVFRTEKKGC GITAELLIPP GEFIMEYVGE VIDSEEFERR QHLYSKDRNRHYYFMALRGEA
SU(Var)3-9 480 VLFKTANGSGW GVRAATALRK NYGNI GEFVCEYIGE IITSDEANER GKAYDDNG--RTYLFDLDYNT
MES-4 1236 LEVVYMNERGF GLVNREPIAV GDFVIEYVGE VINHAEFQRR MEQKQRDR-DENYYFLGVEKDF
CG4565 114 EIFDSPVYGSK GLRTTAKITK GGYICEYAGE LLTVPEARSR LHDNEKLGL-MNYILVLNEYTSDKKQQVT
(MLL1 Y3942F)
TRR mutant Y2404F
TRX mutant Y3701F
PostSET
TRX 3651 VVDATMRGNA ARFINHCCEPNC YSKVVDIL GHKHIIIFAL RRIVQGEELTYDYKFPFEDE KIPCSCGSKRCRKYLN 3726
hMLL1 3892 VVDATMHGNA ARFINHSCEPNC YSRVINID GQKHIVIFAM RKIYRGEELTYDYKFPIEDA SNKLPCNCGAKKCRKFLN 3969
hMLL4 2638 VVDATMHGNA ARFINHSCEPNC FSRVIHVE GQKHIVIFAL RRILRGEELTYDYKFPIEDA SNKLPCNCGAKRCRRFLN 2715
TRR 2354 VVDATLSGGL ARYINHSCNPNC VTEIVEVD RDVRIIIFAK RKIYRGEELSYDYKFDIEDE SHKIPCACGAPNCRKWMN 2431
hMLL2 5460 VIDATLTGGP ARYINHSCAPNC VAEVVTFD KEDKIIIISS RRIPKGEELTYDYQFDFEDD QHKIPCHCGAWNCRKWMN 5537
hMLL3 4834 VIDATLTGGP ARYINHSCAPNC VAEVVTFE RGHKIIISSS RRIQKGEELCYDYKFDFEDD QHKIPCHCGAVNCRKWMN 4911
ySET1 1002 VIDATKKGGI ARFINHCCDPNC TAKIIKVG GRRRIVIYAL RDIAASEELTYDYKFEREKD DEERLPCLCGAPNCKGFLN 1080
SET1 1566 IIDATKCGNL ARFINHSCNPNC YAKVITIE SEKKIVIYSK QPIGINEEITYDYKFPLEDE KIPCLCGAQGCRGTLN 1641
E(Z) 688 VVDATRKGNK IRFANHSINPNC YAKVMMVT GDHRIGIFAK RAIQPGEELFFDYRYGPTEQ LKFVGIEREMEIV 760
ASH1 1444 VIDGQRMGSD CRFVNHSCEPNC EMQKWSVN GLSRMVLFAK RAIEEGEELTYDYNFSLFNP SEGQPCRCNTPQCRGVIG 1521
SET2 1475 VIDATSKGNI SRYINHSCDPNA ETQKWTVN GELRIGFFSV KPIQPGEEITFDYQYLRYGR DAQRCYCEAANCRGWIG 1551
SU(Var)3-9 562 AQDSEYTIDAASHFINHSCDPNL AVFPCWIEHLNVALPHLVFFTLRPIKAGEELSFDYIRADNED(10)RVECRCGADNCRKVLF 635
MES-4 1298 IIDAGPKGNL ARFMNHSCEPNC ETQKWTVN CIHRVGIFAI KDIPVNSELTFNYLWDDLMN NSKKACFCGAKRCSGEIG 1375
CG4565 183 IVDPSRRGNI GRYLNHSCEPNC HIAAVRIDCPIPKIGIFAA RDIAAKEELCFHYGGEGQYKKMTGGKTCLCGASKCTGFMP 263
F/Y switch position

**Fig. S5. Alignment of conserved SET domains.** The TRX SET domain was aligned with eight SET proteins in *Drosophila melanogaster* (in bold), yeast (y) SET1 and human (h) MLL1-4. Eight *Drosophila* SET proteins: TRR, SET1, E(Z), ASH1, SET2, SU(Var)3-9, MES-4, CG4565 was listed in the order of similarity score from the highest at top. Human MLL1 and 4 are orthologs of TRX while MLL2 (ALR) and 3 are orthologs of TRR. Invariant residues are in red (indicated by asterisk at top). Highly conserved (or similar) residues are in magenta color. Residues that are conserved or similar in TRX, TRR and human MLL1-4 are highlighted in blue. Note that TRX Gly (G) 3601 and Glu (E) 3616 are invariant sites and that the TRX Tyr (Y) 3701 at F/Y switch position (indicated at bottom) is replaced by Phe (F) in E(Z), SET2 and SU(var)3-9. The 10 residues omitted in the Post SET of SU(VAR)3-9 are VPYENLSTAV.

**Fig. S6**

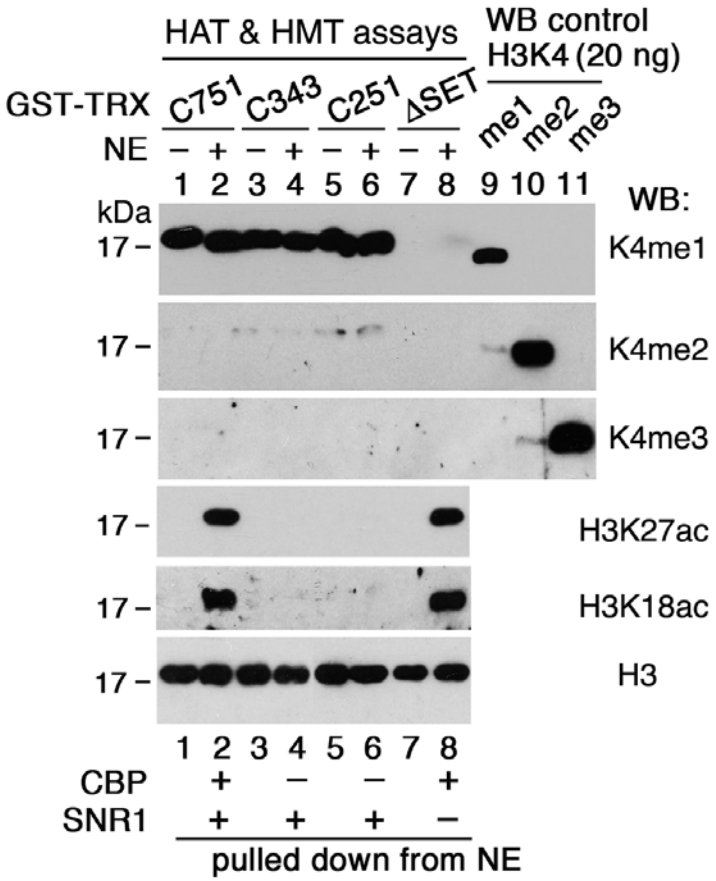


**Fig. S6. A TRX-C complex containing CBP acetylates H3K27 and monomethylates H3K4 in vitro.** GST-TRX-C pull-downs in the presence (+) or absence (–) of nuclear extracts (NE) were used for in vitro HAT and HMT assays. Free recombinant histone H3 was used as substrate and analyzed by Western blots. Recombinant H3K4me1/2/3 (20 ng/lane) were used in lanes 9-11 for positive and negative controls for antibody specificity. GST pull-down results of CBP and SNR1 in Fig. 5 are summarized at bottom. The complex(es) pulled down by TRX-C751 and ΔSET (but not by TRX-C343 and C251) was able to

acetylate H3 on K27 and K18 (see lanes 2, 4, 6 and 8), modifications that we previously showed to be carried out by CBP in vitro and in vivo (Tie et al., 2009), indicating that the complex associating with TRX-C has active CBP histone acetylation activity. TRX-C fragments containing SET domain and complexes formed by them all possess only H3K4 monomethylation activity (lane 1-6, top). H3K4 di- or trimethyltransferase activity was not detected from the TRX complexes with stringent antibody specificity controls (second and third panels). Theses results indicate that other components (such as SNR1 and CBP and unknown proteins) in the TRX complexes do not alter specificity of H3K4 methylation and that H3K4 monomethylation by TRX and histone H3 acetylation by CBP are compatible.

**Fig. S7**

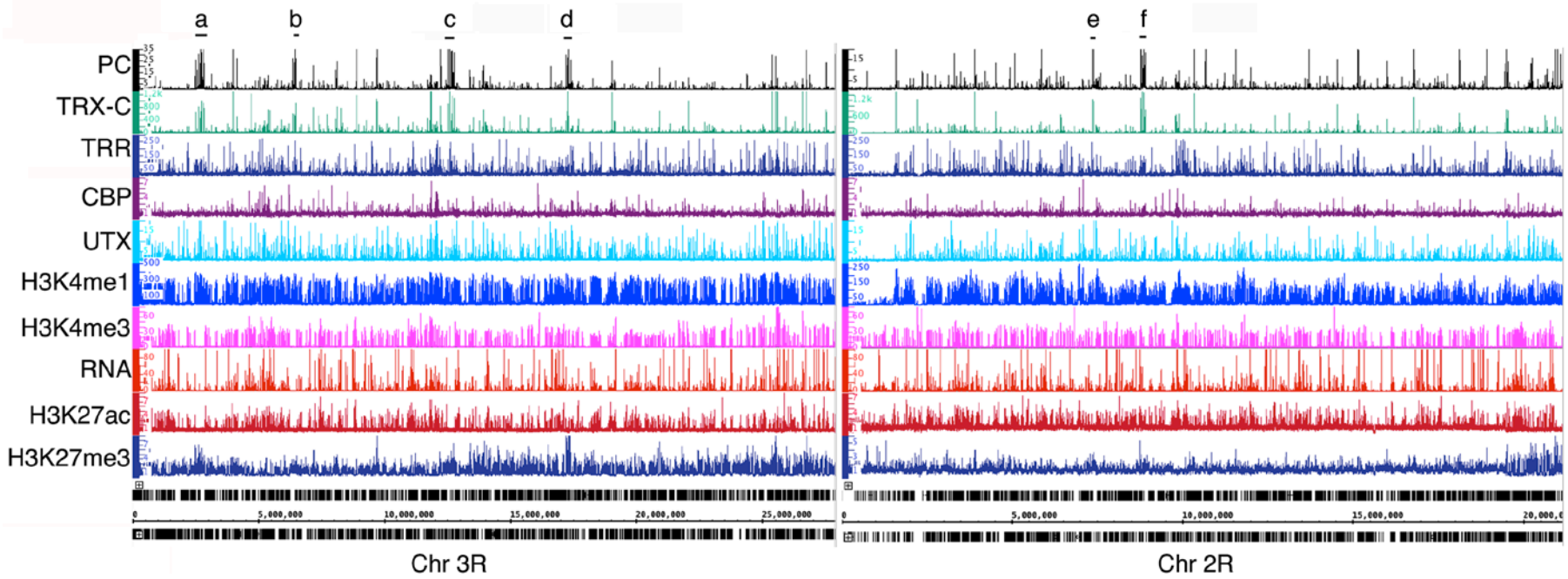


**Fig. S7**. **Strong TRX-C and PC peaks co-localize with peaks of TRR, CBP and H3K4me1 genome-wide.** Plots of ChIP-chip (PC, CBP, UTX, H3K27ac and H3K27me3) (Tie et al., 2012) and ChIP-seq (TRX-C, TRR, H3K4me1, H3K4me3 and RNA) (Enderle et al., 2011; Herz et al., 2012) are displayed at chromosomes 3R and 2R in S2 cells. Six clusters with strong PC binding, marked by a, b, c, d, e and f at top, are the homeotic genes *Antennapedia* Complex (a) and *Bithorax* Complex (c), the homeobox genes *hth* (b), *tin*, *lbl*, *lbe*, *C15* and *slow* (d), *inv* and *en* (e), PcG-regulated genes *vg*, *Psc* and *Su(z)2* (f). Strong TRX-C peaks predominantly co-occupy with strong PC, as well as TRR and CBP at H3K4me1-marked regions (also see Figs S8, S9).

**Fig. S8**

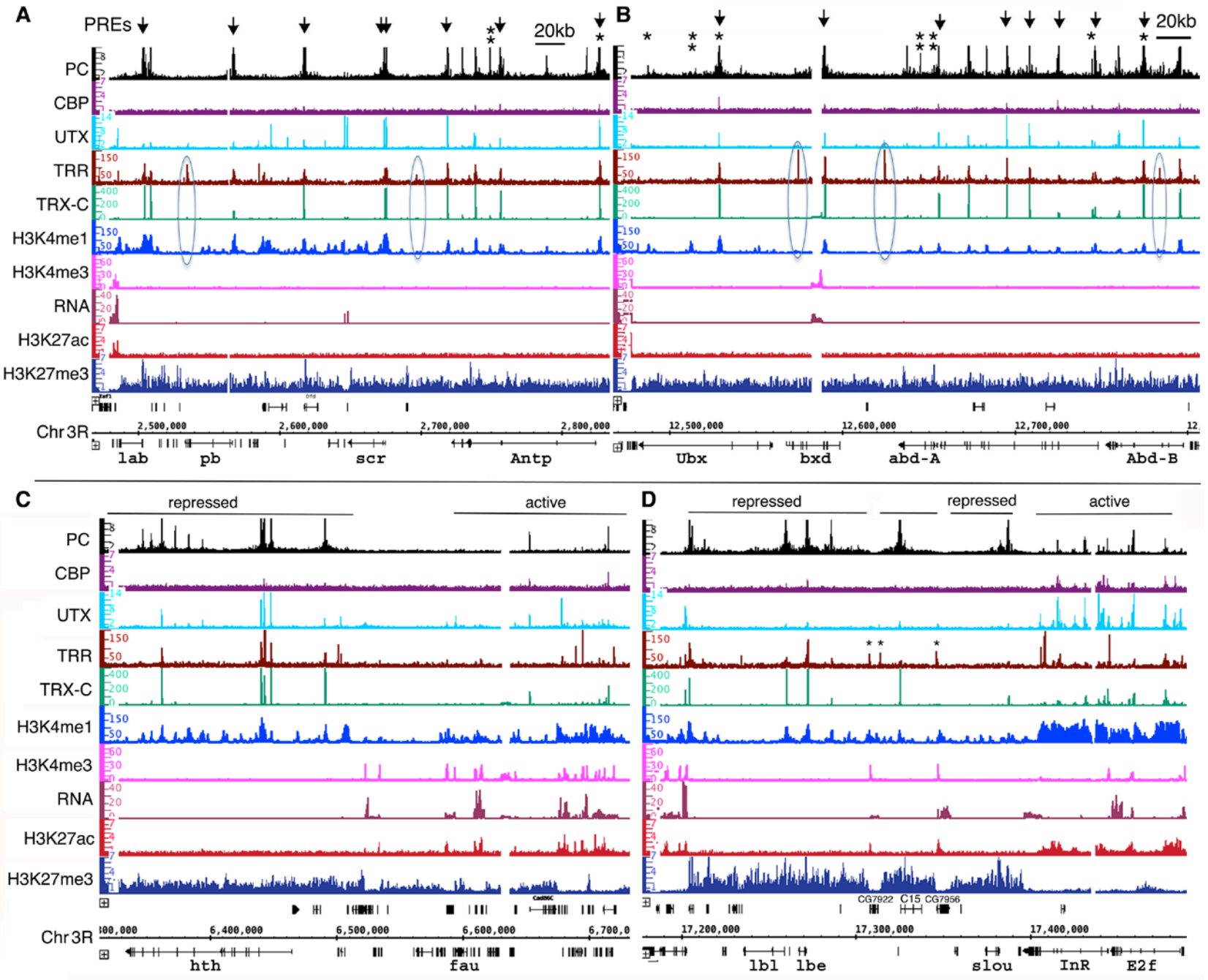
A
PREs
20kb
PC
CBP
UTX
TRR
TRX-C
H3K4me1
H3K4me3
RNA
H3K27ac
H3K27me3
Chr 3R
2,500,000
2,600,000
2,700,000
2,800,000
lab
pb
scr
Antp
B
20kb
12,500,000
12,600,000
12,700,000
Ubx
bxd
abd-A
Abd-B
C
repressed
active
6,400,000
6,500,000
6,600,000
hth
fau
D
repressed
repressed
active
CG7922
C15
CG7956
17,200,000
17,300,000
17,400,000
lbl
lbe
slou
InR
E2f

**Fig. S8. TRX-C is correlated with H3K4me1 at PREs and PcG-regulated genes.** ChIP-chip (Tie et al., 2012) and ChIP-seq (TRX-C, TRR, H3K4me1, H3K4me3 and RNA) plots (Enderle et al., 2011; Herz et al., 2012) are displayed at repressed homeotic genes *Antennapedia* (in A) and *Bithorax* Complexes (in B), homeobox genes *hth* (in C) and *lbl*, *lbe*, *C15* and *slow* (in D) on chromosome 3R in S2 cells. Note that known PREs, marked by arrows at top in A and B and are strongly enriched with PC and H3K27me3, are also enriched with TRX-C and H3K4me1 but are absence of H3K4me3. Also note that H3K4me1 is absent at five TRR peaks (non-PRE sites, circles in A and B), suggesting that TRR is enzymatically inactive at these sites. Enhancers of *Ubx*, *abd-A*, *Abd-B* and *Antp* identified by STARR-seq (Arnold et al., 2013) are indicated by asterisk in A and B. Active genes are enriched by H3K27ac and H3K4me3 but weak TRX-C (see right side in C and D). Scales in A, B, C and D are same. Note that three TRR peaks (marked by asterisk in D) but no TRX peaks are present at active non-PcG targets CG7922 and CG7956.

**Fig. S9**

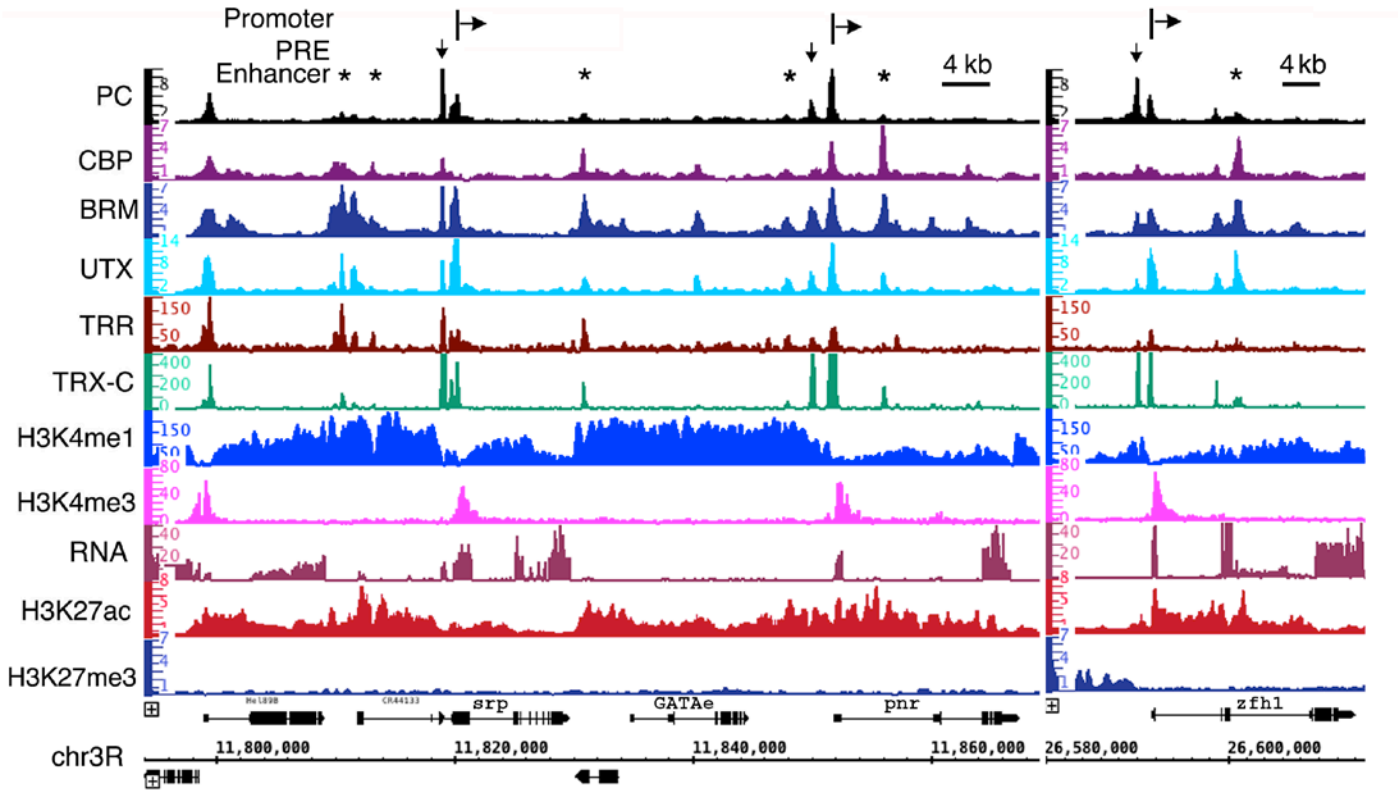


**Fig. S9. TRX-C is enriched at PREs and promoters of active Polycomb target genes.** ChIP-chip and ChIP-seq plots are displayed at Polycomb target genes *srp*, *pnr* and *zfh1* on chromosome 3R in S2 cells. PREs (vertical arrow), Promoter (vertical line at H3K4me3 peak) and known enhancers (asterisk) (Arnold et al., 2013) are marked at top. Horizontal arrows indicate 5′ to 3′ direction for the genes described. Note that RNA and H3K27ac peaks are present at these three active genes. Also note that the distance between PRE and promoter of *srp*, *pnr* and *zfh1* genes is less than 5 kb.

**Fig. S10**

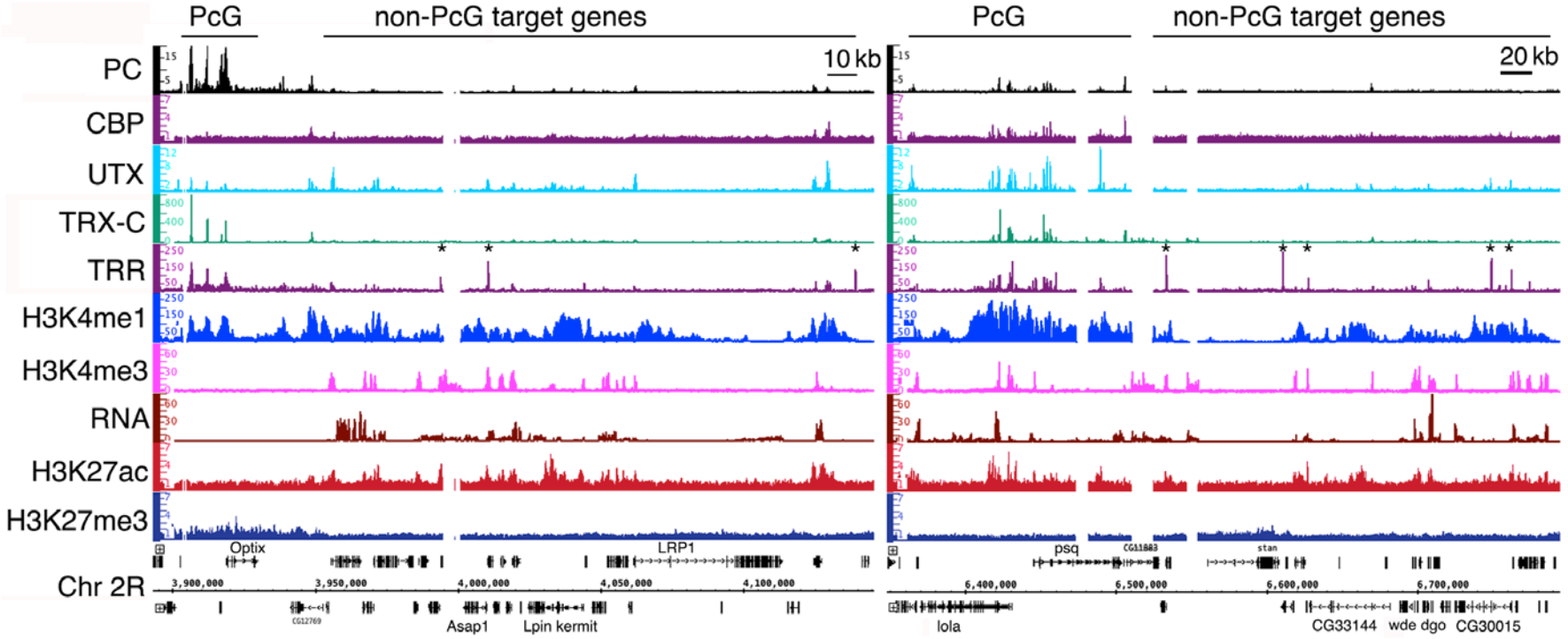


**Fig. S10. TRR is enriched on active non-PcG genes in absence of TRX-C.** Representative plots of ChIP-chip and ChIP-seq are displayed at chromosome 2R in S2 cells. Note that both TRX-C and TRR co-occupy with H3K4me1 and are enriched at repressed PcG gene *Optix* and active PcG genes *lola* and *psq*. However, only TRR (and absence of TRX-C, indicated by asterisk) is enriched on non-PcG genes (marked at top).